

# A kinetic study on bacterial sulfate reduction

L. A. Bernardez · L. R. P. de Andrade Lima ·  
E. B. de Jesus · C. L. S. Ramos · P. F. Almeida

Received: 24 December 2012 / Accepted: 15 April 2013 / Published online: 1 May 2013  
© Springer-Verlag Berlin Heidelberg 2013

**Abstract** The activity of anaerobic sulfate reduction was studied using sulfate-reducing bacteria isolated from the water produced from a Brazilian oil reservoir. The effects of the initial sulfate concentration on the anaerobic sulfate reduction and sulfide generation kinetics were investigated. The redox potential, the biomass solution content, and the sulfate and the sulfide solution content were measured. The results indicate that the sulfate conversion and the sulfide generation are both first-order processes for the initial sulfate concentration of 823, 1,282, and 1,790 mg/L. The results for the kinetic constants for the sulfate conversion indicate an inhibition with the enhancement of the initial sulfate solution content. The kinetic constants for the sulfide generation indicate that this reaction is almost independent of the initial sulfate solution content due to the presence of at least two in-series processes that are faster than the microbial conversion of the sulfate. The kinetic

test using the water from an onshore oil field, with an initial sulfide content of 228 mg/L and sulfate content of 947 mg/L, shows a sulfate conversion of 50 % in 528 h. The kinetic modeling for the net content of sulfate and sulfide indicates that the sulfate conversion is slower for this water than for the deionized water tests; however, the sulfide formation has almost the same conversion velocity. The reactions are first order in both cases.

**Keywords** Souring · Sulfate-reducing bacteria · Sulfide · Kinetics

## Introduction

The generation of hydrogen sulfide ( $H_2S$ ) is a permanent cause of concern in oil production due to the anaerobic corrosion of steel which plugs pipes by precipitation of iron sulfides and also constitutes environment and occupational risk due to the contamination of fuel gas and fuel oil [1–4]. The hydrogen sulfide accumulated in the oil fields could have been generated by bacterial and thermochemical sulfate reduction before field exploration or may be due to the bacterial sulfate reduction during field production [1, 3, 4]. It is important to evaluate the kinetics of sulfate consumption and sulfide generation for a specific population of sulfate-reducing bacteria (SRB) so as to predict and control their activity. This aim of this paper was to investigate the effect of the sulfate concentration on the microbial sulfate reduction and sulfide generation kinetics for simple media, deionized water, and for oil field production water.

The sulfate reduction by SRB follows the reaction described in Eq. 1 below, where the electrons are generated by the oxidation of organic nutrients, the source of carbon and energy for the bacteria [3, 5]:

---

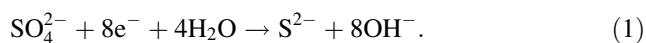
L. A. Bernardez · C. L. S. Ramos · P. F. Almeida  
Department of Bio-Interaction Sciences, Federal University of Bahia, Av. Reitor Miguel Calmon, s/n, Vale do Canela, Salvador, Bahia 40110-902, Brazil  
e-mail: leticiab@ufba.br

C. L. S. Ramos  
e-mail: catia\_larissa@hotmail.com

P. F. Almeida  
e-mail: pfa@ufba.br

L. R. P. de Andrade Lima (✉) · E. B. de Jesus  
Department of Materials Science and Technology, Federal University of Bahia, C.P. 6974, Salvador, Bahia 41810-971, Brazil  
e-mail: lelo@ufba.br

E. B. de Jesus  
e-mail: ebjesus@ufba.br



Studies for microbial sulfate reduction have shown that the reaction kinetic is affected by the feed sulfate, the nutrient solution content, and by the temperature [6–12]. As described in Eq. 1, during sulfate-reducing bacteria growth the pH increases due to the generation of  $\text{OH}^-$  ions and the oxidation–reduction potential of the solution decreases due to the consumption of electrons. The shape of the redox potential curve is characteristic of the type of microorganism and generally the sulfate-reducing bacteria can grow in the culture medium at a range of  $-100$  to  $-500$  mV ( $E_h$ ). By changing the pH the dissolved sulfide can be found as  $\text{S}^{2-}$ ,  $\text{HS}^-$  or  $\text{H}_2\text{S}$ ; however, for the sulfate-reducing bacteria growth range pH, in a non saline solution, the predominant specie is  $\text{HS}^-$ .

In this study the kinetic experiments of the SRB was initially performed in a simple media composed of deionized water and organic nutrients and then using production water from an oil field.

## Materials and methods

### Microbial culture and medium

A volume of 100  $\mu\text{L}$  of mixed culture of SRB, isolated from production water from an oil field, containing about  $2.0 \times 10^9$  MPN/mL was inoculated and enriched in Postgate medium inside the anaerobic chamber (Bactron VI, Shellab, Sheldon Manufacturing Inc.) at 38 °C. The modified Postgate medium, in which sodium lactate is used as a potential carbon source and electron donor, contained (per liter) the following: agar 2.0 g,  $\text{KH}_2\text{PO}_4$  0.5 g,  $\text{NH}_4\text{Cl}$  1.0 g,  $\text{Na}_2\text{SO}_4$  1.0 g,  $\text{CaCl}_2$  1.0 g,  $\text{MgCl}_2 \cdot 6\text{H}_2\text{O}$  1.83 g, yeast extract 1.0 g, ascorbic acid 0.1 g, sodium thioglycollate 0.013 g, sodium citrate 6.38 g, sodium lactate 1.75 mL, NaCl 3.5 %, resazurin 2.0 mL 0.025 % w/v, and  $\text{FeSO}_4 \cdot 7\text{H}_2\text{O}$  0.5 g. All components were dissolved in deionized water and the pH was adjusted to 7.5–8.0 using HCl or NaOH. After this, the solution was homogenized by agitation and later sterilized at 121 °C for 30 min. It supports the growth of a wide spectrum of SRB, encouraging microbial diversity. In this medium, the formation of black precipitate of iron sulfides indicates the bacteria growth and the sulfate reduction.

### Experimental setup

The kinetics was investigated in sealed 250 mL glass bottles. For the experiments with the synthetic medium, in each bottle an equal amount of 200 mL of the previously autoclaved medium, without agar, and 2.0 mL of inoculum were

added and put inside the anaerobic chamber. Then the bottles were continuously mixed in a mechanical shaker at 120 rpm at 38 °C. At certain time intervals, one bottle was selected, aliquots withdrawn, and used for the chemical and biological analysis. The initial concentration of sulfate in the modified Postgate medium was about 1,000 mg/L, but in the kinetic tests the amount of  $\text{Na}_2\text{SO}_4$  and  $\text{FeSO}_4 \cdot 7\text{H}_2\text{O}$  was proportionately modified in the culture medium to reach the concentrations of 823, 1,282, and 1,790 mg/L; the amount of the other components of the culture medium was the same.

For the kinetic experiments using the produced water, in each bottle an equal amount of 200 mL of water and 2.0 mL of the enriched solution were added to allow microbial growth in a period of some weeks. The enriched solution contained (per liter) sodium lactate 1.681 g, sodium citrate 4.411 g, sodium acetate 0.410 g,  $\text{FeSO}_4 \cdot 7\text{H}_2\text{O}$  0.600 g, and toluene 0.525 g. In each bottle 2.0 mL of the inoculum was then added. Then, the bottles were continuously mixed in a mechanical shaker at 120 rpm at 38 °C. At certain time intervals, one bottle was selected, aliquots withdrawn, and used for the chemical and biological analysis.

### Analytical procedures

#### *Sulfate solution content*

The sulfate concentrations were measured by turbidimetric method [13]. This method is based on the precipitation of sulfate ions as barium sulfate. The samples to be analyzed for sulfate were treated with an excess of zinc acetate dehydrate crystals to precipitate dissolved sulfide as zinc sulfide. Fixation of sulfide prevented oxidation to sulfate. Using 1.5 mL microcentrifuged tubes, 1.0 mL culture samples were stirred for 5 s with approximately 0.01 g of zinc acetate. The mixture was then centrifuged for 10 min at 6,000 rpm and at 4 °C. Then 50  $\mu\text{L}$  of the supernatant was mixed with 950  $\mu\text{L}$  of the conditioning fluid in a fresh microcentrifuge tube and stirred for 5 s. Approximately 0.01 g of crushed barium chloride dehydrate crystals was then added to the mixture which was stirred for 15 s and the relative absorbance was immediately read at 420 nm using a UV/Visible spectrophotometer. The calibration standards were prepared using sodium sulfate and deionized water.

#### *Sulfide solution content*

The solution sulfide content was also measured using a turbidimetric method [14]. Measurement had to be done immediately after sampling to prevent its oxidation and volatilization. When copper sulfate is added to a solution containing sulfide, copper sulfide precipitates. The assay is based on this precipitation of colloid copper sulfide because the absorbance of the resulting mixture can be

measured at 480 nm, and it is proportional to sulfide concentration. Using 1.5 mL microcentrifuge tubes, 50  $\mu$ L of the culture samples was mixed with 950  $\mu$ L copper solution (5.0 mM  $\text{CuSO}_4 \cdot 5\text{H}_2\text{O}$  and 50 mM HCl) and then stirred for 5 s. Then the relative absorbance was measured at 480 nm using a spectrophotometer. Calibration standards at 100, 200, 300, 400, 500, 600, and 700 mg/L were produced from the dilution of a standard solution and used to produce a calibration curve.

#### *Solution pH and oxidation–reduction potential*

For the pH measurements a Thermo Orion PerpHecT Meter (Model 330) was used. The pH meter was calibrated using buffer solutions (pH of 4 and 7) regularly. Redox potential differences,  $\Delta E_h$ , were measured ex-situ using an ORP electrode with an internal Ag/AgCl reference electrode from Cole-Parmer. The measurements were calibrated with ORP standard solutions (Analion) of 470 and 220 mV at 20 °C.

#### *Biomass solution content*

The optical density is a classic indication of biomass growth in microbiological processes. In the present case the samples were diluted to appropriate concentrations as needed, and the absorbance of the sample was measured with a spectrophotometer at 600 nm. A calibration curve to relate the absorbance with cell dry weight was then generated. As a rule of thumb, an optical density of one unit corresponds to approximately 1.0 g/L of dry cells.

The dry weight of bacterial mass is another classic indication of the biomass growth in microbiological processes. In this study aliquots of 2.8 mL were transferred to an Erlenmeyer flask containing 250 mL of Postgate's medium. The Erlenmeyer was incubated in an anaerobic environment for 120 h at 38 °C because this is the optimum growth temperatures for the SRB. Aliquots of 45 mL were taken and after 15 min the culture was centrifuged at 10 °C for 20 min at 11,000 rpm. The supernatant was discarded and the biomass washed with 10 mL of deionized water. The suspension was centrifuged at 10 °C for 10 min at 10,000 rpm. The supernatant was again discarded and the biomass was resuspended using 10 mL of deionized water to produce a bacterial mother culture.

From the bacterial mother culture a 1:10 dilution was made (1.0 mL of the mother culture and 9.0 mL of deionized water). From the 1:10 dilution, subsequent dilutions were made and used in the construction of the curve. The dilutions were the following (in duplicate): 1:5, 1:10, 1:15, 1:20, and 1:25. After this, the optical density of the samples and their respective dry weights were analyzed.

Sheets of cellulose acetate filter membrane of 0.22  $\mu$ m pore size supported in an aluminum weighing pan were

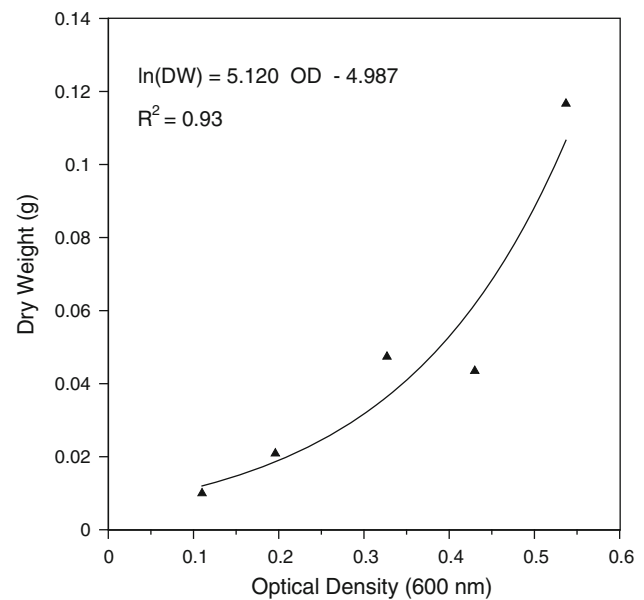


**Fig. 1** The relationship of optical density at 600 nm with dry weight in cell suspensions of SRB

dried in an oven. After this, the sheets were weighed and stored in a desiccator lined with anhydrous  $\text{CaSO}_4$  for 24 h. Then 5 mL of the culture was poured into the holding reservoir fitted on the filter membrane. A vacuum was applied to pull the liquid through the membrane. The reservoir was rinsed with a few mL of water and any paste adhering to the glassware was scraped off. The wet weight of the culture was measured immediately after all the water has been pulled through. The cell mass was dried in an oven set at 105 °C. The weight of the pan/filter plus the cell mass was measured periodically until there was no further decrease in the dry weight. A period of 24 h was necessary to dry the sample completely. Finally, the difference in weight was calculated and the dry weight expressed in g/L. Figure 1 shows the optical density (OD) and dry weight (DW) for the suspensions of SRB. Linear proportionality is true in the region of low concentrations and then there is a deviation due to secondary scattering; therefore, the dilutions are necessary to provide an accurate evaluation of the cell density at high concentrations.

Iron sulfides were used as an indicator of SBR growth. Blackening of the medium due to the formation of iron sulfides were indicative of positive growth. This precipitate could not be readily removed by filtration or centrifugation. The addition of chloride acid to the mixture resulted in a clear solution and the optical measurements could then be performed.

#### *Oil field water sampling*

The samples of production water were collected at an onshore oil field located in the western part of the

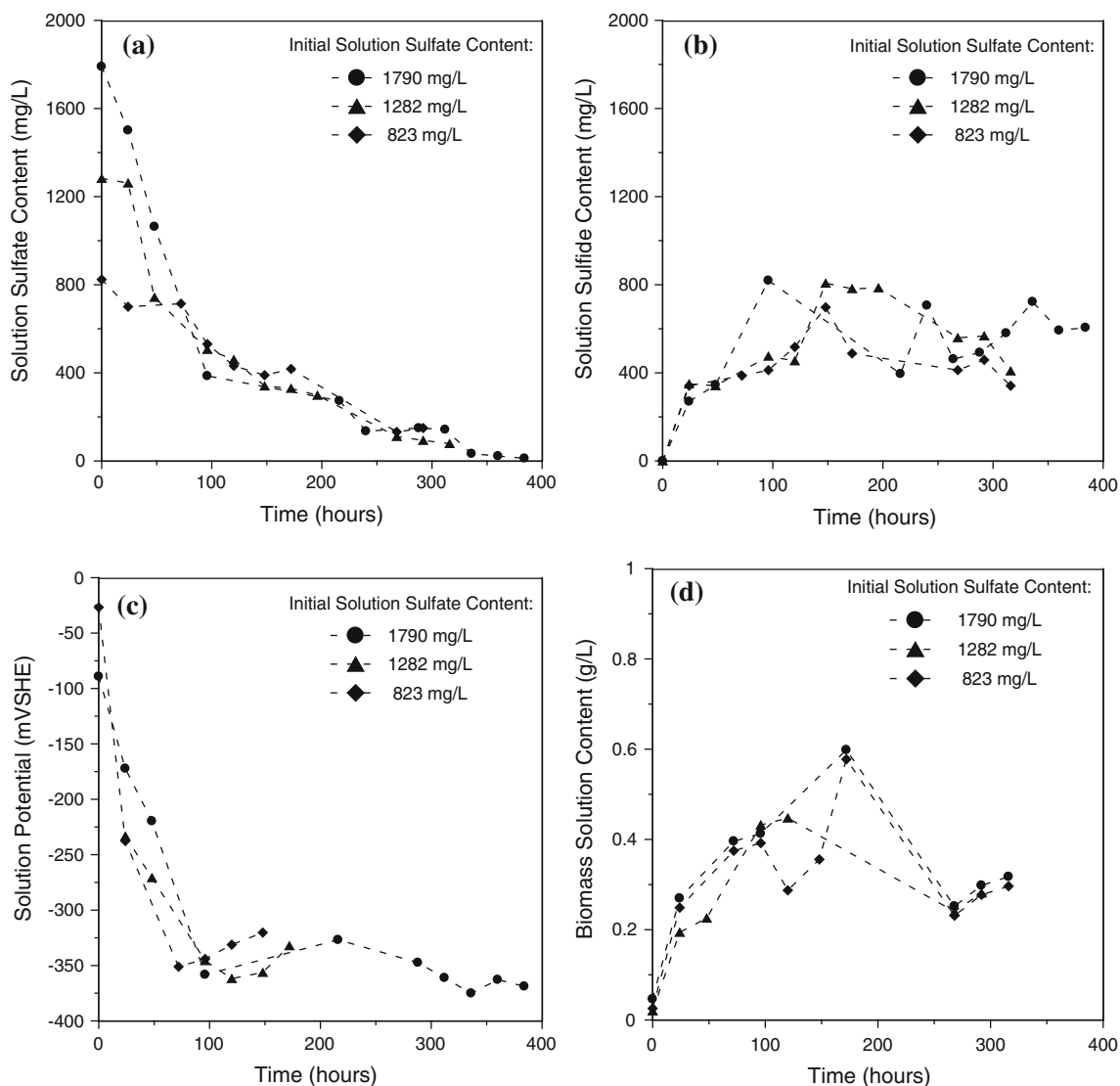


**Fig. 2** Kinetic tests for  $[\text{SO}_4^{2-}]_0 = 823, 1,282, \text{ and } 1,790 \text{ mg/L}$ . **a** Sulfate solution content, **b** sulfide solution content, **c** solution oxidation–reduction potential. **d** Biomass solution content

Recôncavo Basin (Bahia, Brazil) [15]. This field is composed of three main tilted blocks, separated by faults. The main oil reservoirs are in the Sergi formation, consisting of sandstones with some argillaceous intercalations, separating 14 reservoir units over a depth of 200 m and an average thickness of 9 m. The original oil region occupies an area enclosed in rectangle measuring  $2 \times 4 \text{ km}$ . The reservoir has an average porosity of about 22 % and an average initial water saturation of about 24 %, and its permeability ranges from 150 to 900 millidarcies. The reservoir temperature is on average  $44 \text{ }^\circ\text{C}$ , the initial pressure is 55 bar, the oil gravity is  $35^\circ\text{API}$ , and the oil viscosity ranges from 2 to 10 centipoises for the usual range of pressure in reservoir conditions [15]. The population of sulfate-reducing bacteria was

previously isolated from this field. Furthermore, samples were filtered in the laboratory to eliminate solids and large oil particles. The samples were evaporated in an oven and the solid phase was used to analyze the salt composition using X-ray fluorescence and mineralogy phase identification using X-ray diffraction. The pH and oxidation–reduction potential of the solution were measured using conventional electrodes.

#### Kinetic modeling

The batch reactors used in this study have a constant volume and are continuously stirred. Assuming that the mass transfer is fast and the chemical reaction slow, which is likely in this process, the global kinetic models for sulfate

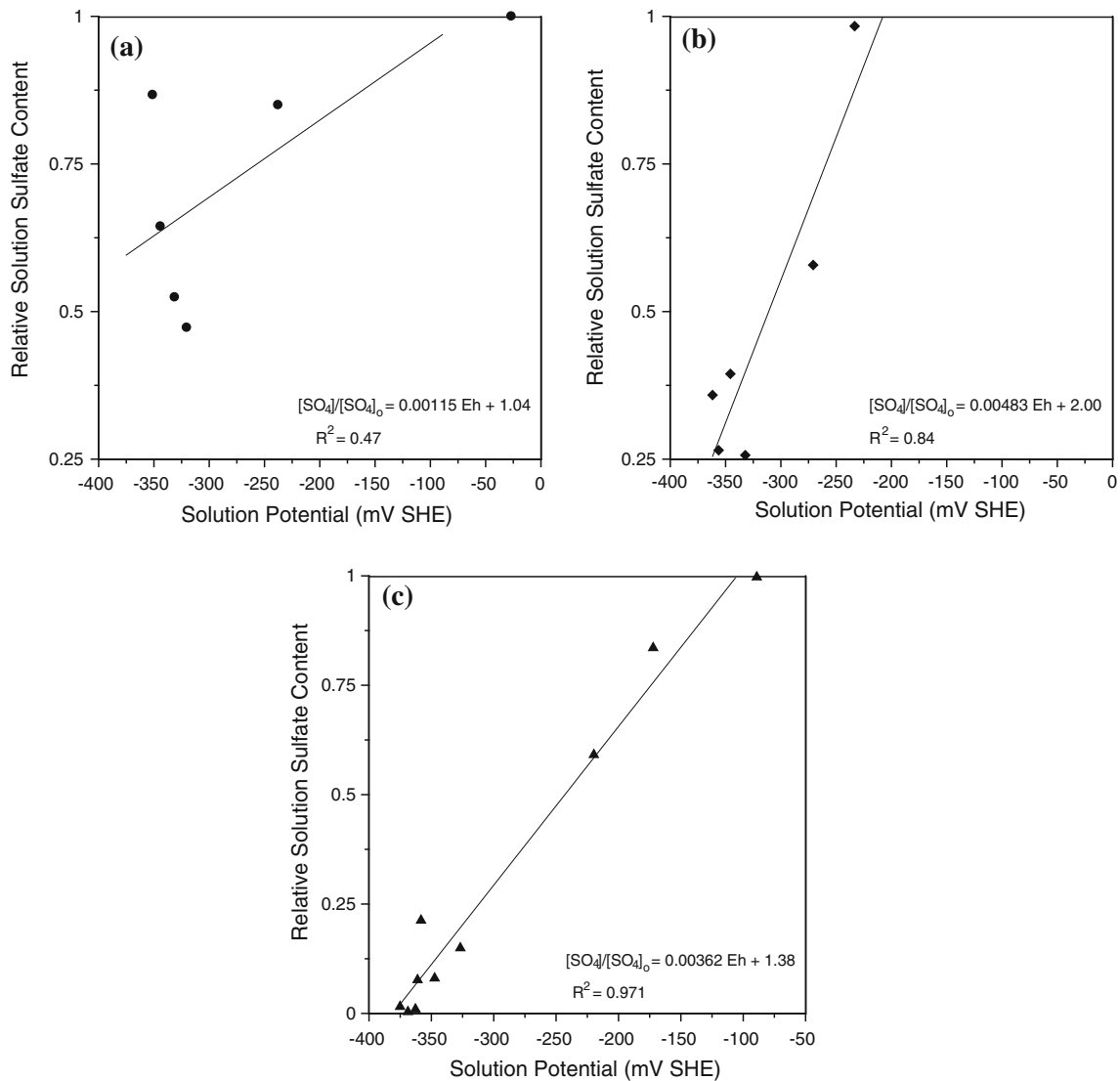


**Fig. 3** Correlation between the solution oxidation–reduction potential and sulfate solution content

consumption and sulfide production can be given by pseudo-homogeneous kinetics as follows [12]:

$$r_{\text{SO}_4^{2-}} = \frac{dC_{\text{SO}_4^{2-}}}{dt} = -k_{\text{SO}_4^{2-}} C_{\text{SO}_4^{2-}}^\alpha \quad (2)$$

$$C_{\text{SO}_4^{2-}}(0) = C_{\text{SO}_4^{2-},0} \quad (3)$$

$$r_{\text{S}^{2-}} = \frac{dC_{\text{S}^{2-}}}{dt} = k_{\text{S}^{2-}} \left( C_{\text{S}^{2-},\infty} - C_{\text{S}^{2-}} \right)^\beta \quad (4)$$

$$C_{\text{S}^{2-}}(0) = 0 \quad (5)$$

where  $C_{\text{SO}_4^{2-}}$  is the solution sulfate content,  $k_{\text{SO}_4^{2-}}$  is the sulfate consumption kinetic constant,  $\alpha$  is the sulfate consumption reaction order,  $C_{\text{SO}_4^{2-},0}$  is the initial solution sulfate content,  $t$  is the time,  $C_{\text{S}^{2-}}$  is the solution sulfide content,  $k_{\text{S}^{2-}}$  is the sulfide generation kinetic constant,  $\beta$  is the sulfide generation reaction order, and  $C_{\text{S}^{2-},\infty}$  is the

final solution sulfate content. In this study, Eqs. 2 and 4 were numerically integrated using the initial conditions given by Eqs. 3 and 5 and the fourth-order Runge–Kutta method. The kinetic parameters ( $k_{\text{SO}_4^{2-}}$ ,  $k_{\text{S}^{2-}}$ ,  $\alpha$ ,  $\beta$ ,  $C_{\text{S}^{2-},\infty}$ ) were evaluated by curve fitting using nonlinear least square.

### Results and discussion

Kinetics of microbial sulfate reduction in a solution of deionized water

Figure 2a, b shows the results for the sulfate consumption and the sulfide production time evolution for the initial solution sulfate content of 823, 1,283, and 1,790 mg/L.

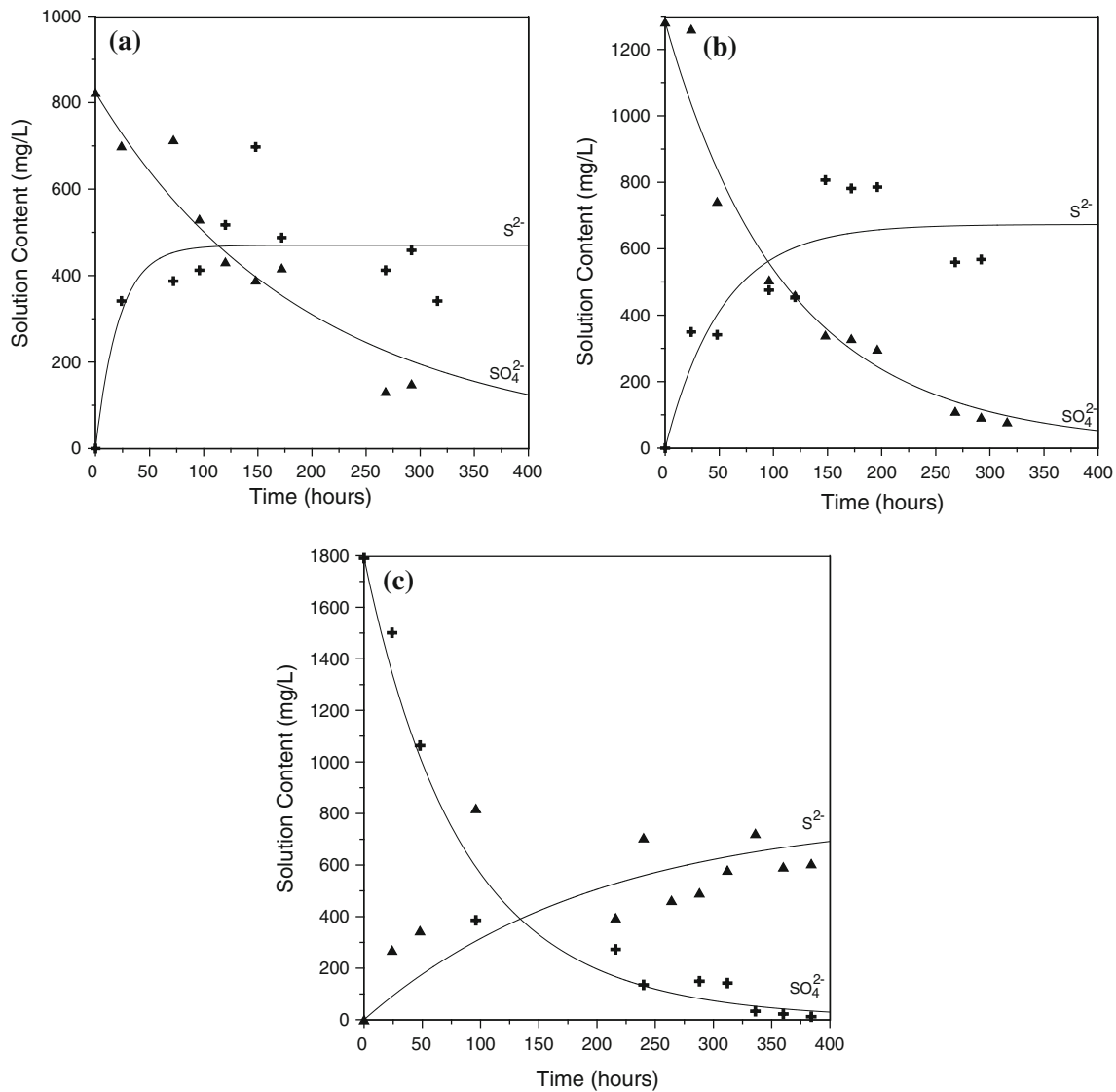


**Fig. 4** Kinetic model fitting for the sulfate and sulfide solution content: **a**  $[SO_4^{2-}]_0 = 823$  mg/L, **b**  $[SO_4^{2-}]_0 = 1,282$  mg/L and **c**  $[SO_4^{2-}]_0 = 1,790$  mg/L

**Table 1** Sulfate conversion kinetic parameters

$C_{SO_4^{2-},0}$ (mg/L)	$k_{SO_4^{2-}}$ [(mg/L) $^{1-\alpha}$ /h]	$\alpha$	$k_{S^{2-}}$ (1/h)	$\beta$	$C_{S^{2-},\infty}$ (mg/L)
823	$-3.16 \times 10^{-3}$	1.1	$4.6 \times 10^{-2}$	1.0	470
1,282	$-5.43 \times 10^{-3}$	1.1	$1.9 \times 10^{-2}$	1.0	673
1,790	$-6.92 \times 10^{-3}$	1.1	$3.0 \times 10^{-3}$	1.0	800

The sulfate solution content decreased rapidly at the beginning and thereafter slowly. The sulfide production is almost independent of the initial sulfate solution content and increased reaching a maximum value near 600 mg/L. At the beginning of the experiment, the pH was relatively constant at 7.5. Therefore, the measured sulfide content represents only the  $S^{2-}$  ion and cannot account for  $HS^-$ ,

$H_2S$ , and other species generated by the ionic equilibrium, which explains the apparent sulfur mass imbalance and agrees with results reported in a previous study [9]. The sulfate conversion ( $\alpha = \left(1 - [SO_4^{2-}] / [SO_4^{2-}]_0\right) \times 100$ ) over a period of 288 h for the initial sulfate content of 823, 1,283, and 1,790 mg/L was 82, 88, and 92 %, respectively.

Figure 2c shows the solution oxidation–reduction potential time evolution. The redox potential curves have analogous shapes to the sulfate conversion curves (Fig. 2a) with a rapid reduction at the beginning and thereafter a slow reduction. In the end it stabilizes near  $-350$  mV. Figure 2d shows the optical density solution content time evolution, which indicates the growth of bacteria biomass.

Figure 3 shows the correlation between the solution oxidation–reduction potential and the sulfate solution using the data presented in Fig. 2a–c. The results show a correlation between the solution potential and the sulfate conversion in sulfide which increases with the sulfate solution content. The correlation for low initial sulfate concentration is moderated due to the limitation of the analytical methods. However, for larger initial sulfate concentrations the correlation is strong. These results show an indication to evaluate the activity of the SRB in a system.

Figure 4a, b, c shows the resulting kinetic modeling for the sulfate and sulfide solution content for the three cases using Eqs. 2 and 4. The kinetic parameters are presented in Table 1. It can be seen that the reaction order in all cases is near one, the sulfate consumption kinetic constants increase with the enhancement of the sulfate content of the solution, and the kinetic constants for the sulfide production decreases with the enhancement of the initial solution sulfate content. The rate constants can be correlated with the initial sulfate solution content using the following equations:

$$k_{SO_4^{2-}} = 2.939 \times 10^{-2} - 4.854 \times 10^{-3} \ln C_{SO_4^{2-},0} \quad (6)$$

$$k_{S^{2-}} = 4.187 \times 10^{-1} - 5.564 \times 10^{-2} \ln C_{SO_4^{2-},0} \quad (7)$$

$$C_{S^{2-},\infty} = 4.265 \times 10^2 \ln C_{SO_4^{2-},0} - 2.389 \times 10^3 \quad (8)$$

These results are different from the previously reported kinetic constants [12] due to the fact that in the present case the reactions took place in a batch stirred reactor, and the initial sulfate concentration is lower than that in the previous study.

#### Characterization of the oil field production water

The characterization of the production water from the wells of the onshore oil field indicated that the total dissolved solids range between 0.14 and 0.38 %, the pH ranges between 7.0 and 7.9, and the oxidation–reduction potential ( $E_h$ ) is about  $-100.6$  mV. The water salinity is very low and the pH almost neutral. However, it was noted during the sampling campaigns that there was a significant emanation of  $H_2S$ , which can be explained by the solubility reduction due to the pressure and temperature changes.

Table 2 shows the results of the analysis of the dissolved solids by XRF. Despite the fact that a low-molecular-weight element (such as Na, Si, Cl, C, O, S) could not be detected, the result indicates a Ca content of 110.6 mg/L and a K content of 6.0 mg/L. Figure 5 shows the X-ray diffraction pattern of the dissolved solids that shows that the major phases are halite (NaCl) and calcite ( $CaCO_3$ ). These results can be explained by the water interaction

with the reservoir rock, mainly sandstones with some argillaceous intercalations.

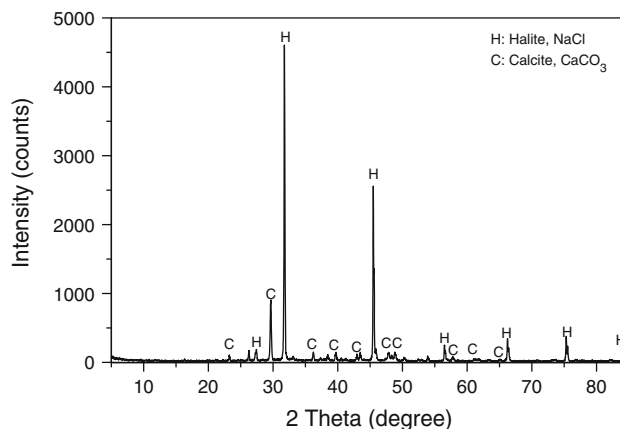
#### Kinetics of microbial sulfate reduction in a solution of oil field production water

Figure 6a–c shows the kinetic test for the produced water. Figure 6a shows the solution oxidation–reduction potential time evolution. Figure 6b shows the optical density solution content time evolution. Figure 6c shows the sulfate and the sulfide solution content time evolution. The water has an initial sulfide content of 228 mg/L and the sulfate content is 947 mg/L. The solution redox potential decreases to a value below  $-350$  mV and the biomass solution content increases accordingly. Then, the sulfate solution content decreases to 477 mg/L; after about 288 h the sulfate conversion is 41 %, and after 528 h it is 50 %.

Figure 7 shows the kinetic modeling for the net content of sulfate and sulfide for the produced water. Table 3

**Table 2** Produced water element content

	Evaporated solid content (mg/kg)	Estimated solution content (mg/L)
Ca	79,400	110.6
K	4,272	5.95
Ba	2,364	3.29
Sr	1,085	1.51
Mn	781	1.09
Te	642	0.89
Rb	414	0.58
Cs	266	0.37
Sb	206	0.29
Sn	145	0.20
Th	88	0.12
Fe	84	0.12



**Fig. 5** Produced water dissolved solids X-ray diffraction pattern

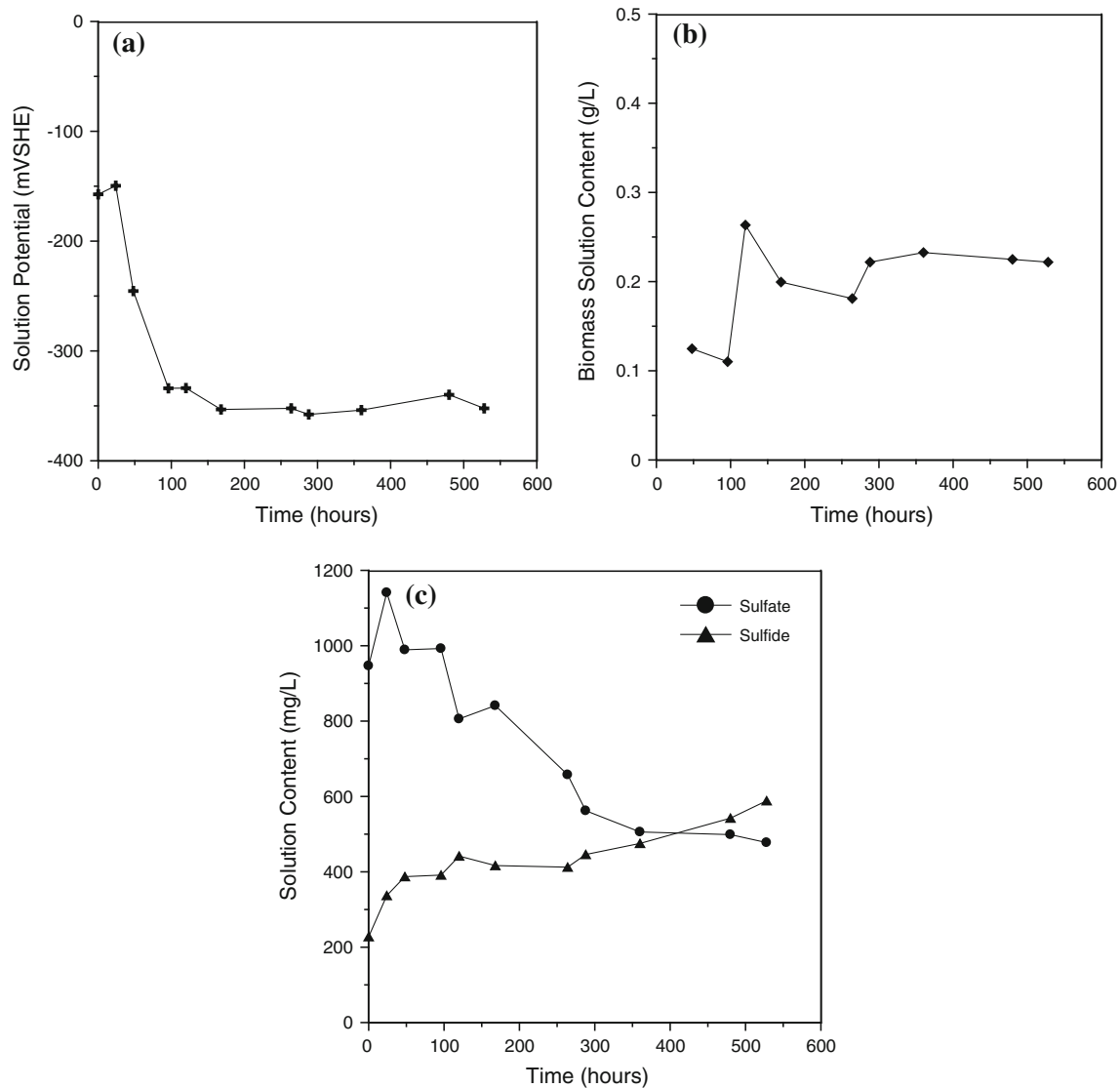


**Fig. 6** Kinetic test for the produced water: **a** Solution oxidation–reduction potential time evolution. **b** Optical density solution content time evolution. **c** Sulfate and sulfide solution content time evolution

shows the resulting kinetic model parameters using Eqs. 2 and 4. The kinetic constants ( $k_{\text{SO}_4^{2-}}$  and  $k_{\text{S}^{2-}}$ ) indicate that the sulfate conversion is slower for the production water than for the deionized water tests, but the sulfide formation is almost the same. Also the reaction orders are the same in both cases, first order.

## Conclusions

This study investigated the activity of a mixed SRB culture collected from a Brazilian onshore oil field. The effects of the initial sulfate concentration of 823, 1,282, and 1,790 mg/L on the anaerobic sulfate reduction and sulfide generation kinetics were investigated in a batch reactor

using deionized water and an enriched culture medium. The redox potential and bacterial growth were also used to monitor the growth and the activity of the SRB throughout the experimental runs. The results indicate that sulfate conversion and sulfide generation are both first-order processes. The kinetic constants for sulfate conversion and sulfide generation indicate an enhancement with the initial sulfate concentration. The reactions are given by  $r_{\text{SO}_4^{2-}} = (2.939 \times 10^{-2} - 4.854 \times 10^{-3} \ln C_{\text{SO}_4^{2-},0}) C_{\text{SO}_4^{2-}}^{1.1}$  and  $r_{\text{S}^{2-}} = (4.187 \times 10^{-1} - 5.564 \times 10^{-2} \ln C_{\text{SO}_4^{2-},0}) [(4.265 \times 10^2 \ln C_{\text{SO}_4^{2-},0} - 2.389 \times 10^3) - C_{\text{S}^{2-}}]^{1.0}$ . The kinetic test performed with the water from the onshore oil field shows in 528 h a sulfate conversion of 50 %. The kinetic



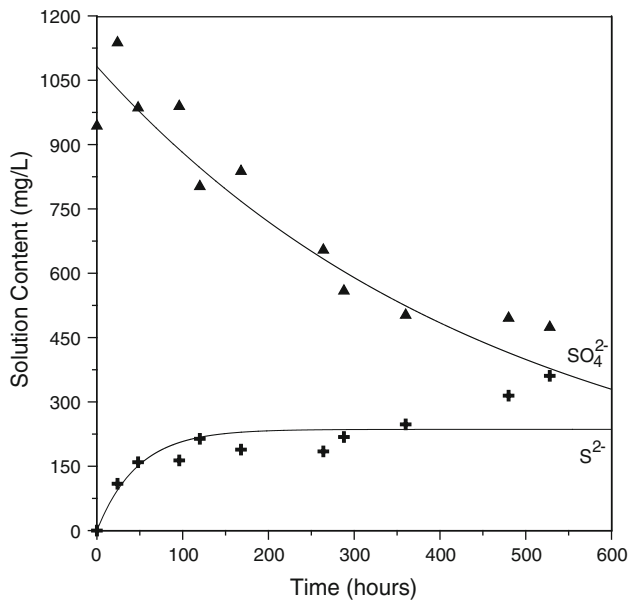


**Fig. 7** Kinetic model fitting for the sulfate and sulfide produced water content

**Table 3** Produced water sulfate conversion kinetic parameters

$C_{SO_4^{2-},0}$ (mg/L)	$k_{SO_4^{2-}}$ [(mg/L) <sup>1-<math>\alpha</math>]/h]</sup>	$\alpha$	$k_{S^{2-}}$ (1/h)	$\beta$	$C_{S^{2-},\infty}$ (mg/L)
1,082	$-1.3 \times 10^{-3}$	1.1	$2.1 \times 10^{-2}$	1.0	236

modeling indicated that the sulfate conversion is slower for the produced water than for the deionized water tests, but the sulfide formation has almost the same conversion velocity.

**Acknowledgments** This research was supported by the *Conselho Nacional de Desenvolvimento Científico e Tecnológico* (CNPq, Brazil) (Project numbers: 480181/2011-0, 309707/2010-2, 302024/2011-5 and 550537/2009-0), Financiadora de Estudos e Projetos (FINEP) and Petróleo Brasileiro S.A. (PETROBRAS) (Project numbers FINEP 0.1.05.0974.00/PETROBRAS 0050. 001843106.4/SAP contract number 4600202295). L.A. Bernardez thanks the Fundação de Amparo a Pesquisa do Estado da Bahia (FAPESB, Brazil) for a fellowship. E.B. de Jesus thanks the CNPq and C.L.S Ramos the FAPESB for graduate scholarships for this project.

**References**

1. Cord-Ruwisch R, Kleinitz W, Widdel F (1987) Sulfate-reducing bacteria and their activities in oil production. *J Petrol Technol* 39:97–106
2. Lizama HM, Sankey BM (1993) On the use of bleach soaks to control bacteria-mediated formation souring. *J Petrol Sci Eng* 9:145–153
3. Vance I, Thrasher DR (2005) Reservoir souring: mechanisms and prevention. In: Magot M, Ollivier B (eds) *Petroleum microbiology*. ASM Press, Washington, pp 123–142
4. Zhu G, Zhang S, Huang H, Liu Q, Yang Z, Zhang J, Wu T, Huang Y (2010) Induced H<sub>2</sub>S formation during steam injection recovery process of heavy oil from the Liaohe Basin, NE China. *J Petrol Sci Eng* 71:30–36
5. Lenz P, Vallero M, Esposito G, Zandvoort M (2002) Perspectives of sulfate reducing bioreactors in environmental biotechnology. *Rev Environ Sci Biotechnol* 1:311–325
6. Nemati M, Jenneman GE, Voordouw G (2001) Mechanistic study of microbial control of hydrogen sulfide production in oil reservoirs. *Biotechnol Bioeng* 74:424–434
7. Moosa S, Nemati M, Harrison STL (2002) A kinetic study on anaerobic reduction of sulfate. Part I. Effect of sulfate concentration. *Chem Eng Sci* 57:2773–2780
8. Moosa S, Nemati M, Harrison STL (2005) A kinetic study on anaerobic reduction of sulfate. Part II. Incorporation of temperature effects in the kinetic model. *Chem Eng Sci* 60:3517–3524
9. Baskaran V, Nemati M (2006) Anaerobic reduction of sulfate in immobilized cell bioreactors, using a microbial culture originated from an oil reservoir. *Biochem Eng J* 31:148–159
10. Al-Zuhair S, El-Naas MH, Al-Hassani H (2008) Sulfate inhibition effect on sulfate reducing bacteria. *J. Biochem. Tech.* 1: 39–44
11. Oyekola OO, van Hille R, Harrison STL (2010) Kinetic analysis of biological sulphate reduction using lactate as carbon source and electron donor: effect of sulphate concentration. *Chem Eng Sci* 65:4771–4781
12. Bernardez LA, de Andrade Lima LRP, Ramos CLS, Almeida PF (2012) A kinetic analysis of microbial sulfate reduction in an upflow packed-bed anaerobic bioreactor. *Mine Water Environ* 31:62–68
13. Kolmert Å, Wikström P, Hallberg KB (2000) A fast and simple turbidimetric method for the determination of sulfate in sulfate-reducing bacterial cultures. *J Microbiol Methods* 41:179–184
14. Cord-Ruwisch R (1985) A quick method for the determination of dissolved and precipitated sulfides in cultures of sulfate-reducing bacteria. *J Microbiol Methods* 4:33–36
15. Estublier A, Dino R, Schinelli MC, Barroux C, Beltran AM (2011) CO<sub>2</sub> injection in Buracica -long-term performance assessment. *Energy Procedia* 4:4028–4035